JCB Article

AIP is a mitochondrial import mediator that binds to both import receptor Tom20 and preproteins

Masato Yano, Kazutoyo Terada, and Masataka Mori

Department of Molecular Genetics, Graduate School of Medical Sciences, Kumamoto University, Kumamoto 860-8556, Japan

Most mitochondrial preproteins are maintained in a loosely folded import-competent conformation by cytosolic chaperones, and are imported into mitochondria by translocator complexes containing a preprotein receptor, termed translocase of the outer membrane of mitochondria (Tom) 20. Using two-hybrid screening, we identified arylhydrocarbon receptor–interacting protein (AIP), an FK506-binding protein homologue, interacting with Tom20. The extreme COOH-terminal acidic segment of Tom20 was required for interaction with tetratricopeptide repeats of AIP. An in vitro import assay indicated that AIP prevents preornithine transcarbamylase from the loss of import competency. In cultured cells, overexpression of AIP enhanced preornithine transcarbamylase import, and depletion of AIP by RNA interference impaired the import. An in vitro binding assay revealed that AIP specifically binds to mitochondrial preproteins. Formation of a ternary complex of Tom20, AIP, and preprotein was observed. Hsc70 was also found to bind to AIP. An aggregation suppression assay indicated that AIP has a chaperone-like activity to prevent substrate proteins from aggregation. These results suggest that AIP functions as a cytosolic factor that mediates preprotein import into mitochondria.

Introduction

Mitochondrial proteins are initially synthesized on cytosolic ribosomes as preproteins with mitochondrial targeting and import signals. During or after synthesis in the cytosol, mitochondrial preproteins associate with chaperones that maintain preproteins in a loosely folded translocation-competent conformation. In yeast, an Hsp70 family member (Ssz1p) and a DnaJ homologue (zuotin) form a ribosome-associated complex that stimulates the translocation of preproteins into mitochondria (Gautschi et al., 2001, 2002). Also in mammals, Hsp70 family member Hsc70 and DnaJ homologues dj2 and/or dj3 are involved in mitochondrial protein import (Terada et al., 1995, Terada and Mori, 2000). The preproteins are then targeted to the mitochondria and imported into the organelle. A dynamic protein complex, termed translocase of the outer membrane of mitochondria (Tom), is responsible for recognizing and translocating preproteins into the organelle. The complex includes the import receptors Tom20 and Tom70, a general import pore that contains an import receptor Tom22, channel protein Tom40, and small Toms (Lithgow et al., 1995; Lill et al., 1996; Neupert, 1997; Mori and Terada, 1998; Herrmann and Neupert, 2000; Pfanner and Geissler, 2001). Preproteins with NH_2-terminal presequences are initially recognized by the receptor Tom20, although preproteins with internal targeting signals such as carrier proteins are recognized preferentially by Tom70. Preproteins bind to the import receptors Tom20 or Tom70 at the mitochondrial surface and are subsequently transferred to the general import pore. Recently, Tom70 was found to be a chaperone-docking protein for the import of Tom70-dependent preproteins (Young et al., 2003). However, no factor that mediates the import of Tom20-dependent preproteins has been reported.

Human Tom20 (hTom20) consists of five segments: an NH_2-terminal membrane anchor segment, a linker segment rich in charged amino acids, a tetratricopeptide repeat (TPR) motif, a glutamine-rich segment, and a COOH-

Address correspondence to Masato Yano, Department of Molecular Genetics, Graduate School of Medical Sciences, Kumamoto University, Honjo 1-1-1, Kumamoto 860-8556, Japan. Tel.: 81-96-373-5140. Fax: 81-96-373-5145. email: myano@gpo.kumamoto-u.ac.jp; or Masataka Mori, Department of Molecular Genetics, Graduate School of Medical Sciences, Kumamoto University, Honjo 1-1-1, Kumamoto 860-8556, Japan. Tel.: 81-96-373-5140. Fax: 81-96-373-5145.
email: masa@gpo.kumamoto-u.ac.jp.

Key words: chaperone; import competency; protein targeting; mitochondria; Tom20

Abbreviations used in this paper: AhR, arylhydrocarbon receptor; AIP, arylhydrocarbon receptor–interacting protein; ECHS1, enoyl-coenzyme A hydratase 1 precursor; FKBP52, 52-kD FK506-binding protein; hTom20, human Tom20; MBP, maltose-binding protein; NDUFB10, NADH: ubiquinone oxidoreductase 1β subcomplex 10; OTC, ornithine transcarbamylase; pOTC, preornithine transcarbamylase; PPIase, peptidyl-prolyl cis/trans isomerase; siRNA, small interfering RNA; Tom, translocase of the outer membrane of mitochondria; TPR, tetratricopeptide repeat.

terminal segment (Goping et al., 1995). TPR is thought to mediate diverse protein–protein interactions (Goebl and Yanagida, 1991). The structure of the cytosolic domain of Tom20 complexed with presequence peptide was analyzed using nuclear magnetic resonance (Abe et al., 2000). The binding groove of Tom20 mainly consists of a TPR and a glutamine-rich segment, and hydrophobic residues in the groove interact with the hydrophobic face of the amphiphilic helical presequence. On the other hand, the role of the COOH-terminal segment in Tom20, which contains conserved acidic residues in higher eukaryotes, is unknown.

In the present work, we performed two-hybrid screening to identify Tom20-interacting proteins. By stepwise screening using two kinds of COOH-terminal region of Tom20 as bait, we isolated arylhydrocarbon receptor (AhR)–interacting protein (AIP), also known as ARA9 and XAP2 (Carver and Bradfield, 1997; Ma and Whitlock, 1997; Meyer et al., 1998). AIP was originally identified to be a component of the mature AhR complex (Carver and Bradfield, 1997; Ma and Whitlock, 1997), and also as a protein interacting with human hepatitis B virus X-protein (Meyer et al., 1998). AIP belongs to a family of peptidyl-prolyl cis/trans isomerases (PPIases) that are ubiquitous in prokaryotes and eukaryotes (Galat and Metcalfe, 1995). PPIase activity has been shown to function in the folding of a number of proteins (Lang et al., 1987). 52-kD FK506-binding protein (FKBP52) also belongs to PPIase. Both AIP and FKBP52 contain three TPR motifs responsible for the binding to Hsp90 (Young et al., 1998; Bell and Poland, 2000). As TPR motifs of FKBP52 have chaperoning activity to prevent proteins from aggregation (Bose et al., 1996; Pirkl et al., 2001), we hypothesized that AIP may have a chaperone-like activity and be involved in mitochondrial preprotein import.

Using two-hybrid analysis and an in vitro binding assay, we found the extreme COOH-terminal acidic segment of Tom20 to be responsible for interacting with TPR motifs in AIP. By in vitro import assay, AIP was found to prevent preornithine transcarbamylase (pOTC) from the loss of import competency. In cultured cells, overexpression of AIP enhanced the pOTC import, and depletion of AIP impaired the import. AIP specifically bound to mitochondrial preproteins. AIP exhibited a chaperone-like activity to suppress the aggregation of substrate proteins. Complex formation among preprotein, AIP, and Tom20 was also observed, and interactions in the complex are also described. We propose that AIP functions as a newly identified factor in the mitochondrial import of Tom20-dependent preproteins.

Results

The extreme COOH-terminal segment of Tom20 specifically binds to AIP

To identify proteins that interact with Tom20, we performed two-hybrid screening using plasmids expressing LexA-(101–145)hTom20 and LexA-(126–145)hTom20 (Fig. 1 A). About 10^7 clones of a human fetal liver library were screened for interaction with region 101–145 of Tom20. 86 clones were recovered as positive ones, and cDNAs extracted from the clones were classified into 16 representatives, then further screened for interaction with re-

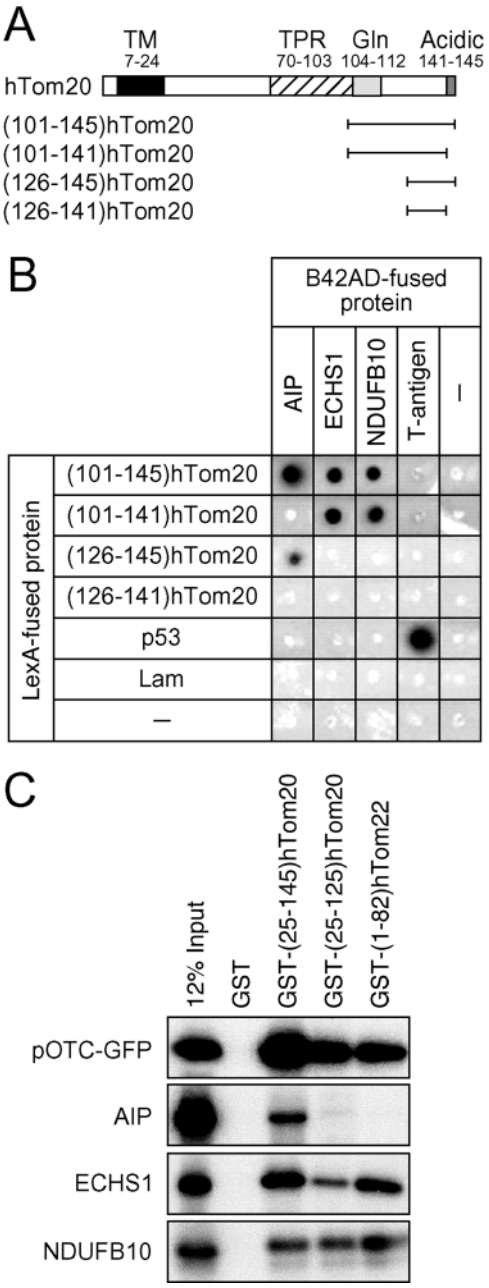

Figure 1. **AIP binds to the extreme COOH-terminal segment of hTom20.** (A) The schematic structures of hTom20 and its deletion mutants fused with LexA are shown. TM, predicted transmembrane domain; TPR, tetratricopeptide repeat motif; Gln, glutamine-rich segment; Acidic, the segment rich in acidic residues. (B) Plasmids expressing LexA-fused hTom20s and B42AD-fused proteins were cotransformed into yeast EGY48[p8op-lacZ] cells. The yeast cells were cultured on indicator medium containing 5-bromo-4-chloro-3-indolyl-D-galactoside. Blue color (seen here in black) indicates a specific interaction in the two-hybrid system. Interaction between p53 and T-antigen was also monitored as positive control. Human lamin C [66–230] (Lam) was used as negative control. ECHS1, mitochondrial short-chain enoyl-coenzyme A hydratase 1 precursor; NDUFB10, mitochondrial NADH:ubiquinone oxidoreductase 1β subcomplex 10. (C) Translation product (10 μl) containing ^{35}S-labeled pOTC-GFP, AIP, ECHS1, or NDUFB10 was incubated with glutathione-Sepharose beads prebound with GST, GST-(25–145)hTom20, GST-(25–125)hTom20, or GST-(1–82)hTom22 (0.6 nmol). After washing, GST derivatives and bound proteins were eluted and analyzed by SDS-PAGE and fluorography. 12% Input: 12% of input ^{35}S-labeled proteins.

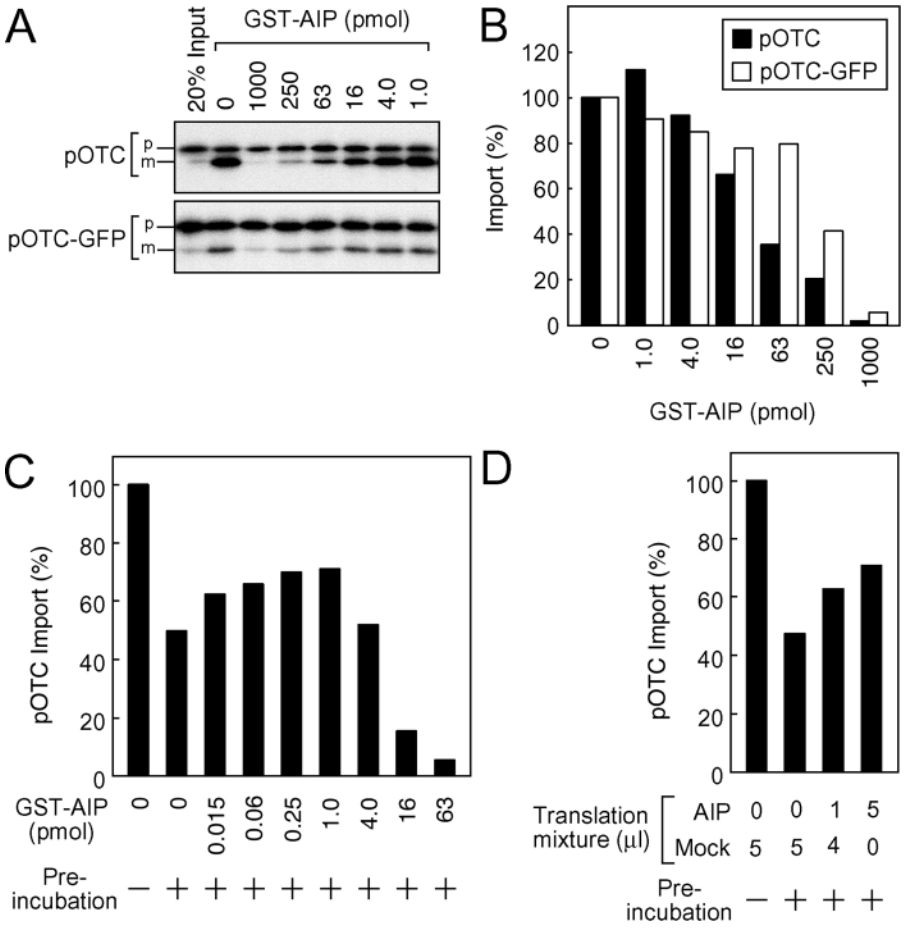

Figure 2. **AIP maintains the import competency of pOTC in vitro.** (A) ^{35}S-labeled human pOTC or pOTC-GFP translated in 10 μl reticulocyte lysate was mixed with 25 μg isolated mitochondria in the presence of indicated amounts of purified GST-AIP in the import reaction mixture (total, 50 μl). After a 20-min incubation at 25°C, the import reaction was stopped, and reisolated mitochondria were subjected to SDS-PAGE and fluorography. 20% Input; 20% of input ^{35}S-labeled preproteins; p and m, precursor and mature forms, respectively. (B) The radioactive cleaved mature proteins shown in A were quantified. The percentage of import represents the amount of mature proteins compared with controls without GST-AIP. (C) ^{35}S-labeled human pOTC translated in 5 μl reticulocyte lysate was mixed with indicated amounts of GST-AIP in the import reaction mixture without mitochondria (total, 90 μl), and the mixture was incubated at 25°C for 20 min (preincubation). The mixture was then mixed with isolated mitochondria (total, 100 μl). The import reaction and quantification were done as in A and B. The percentage of import represents the amount of mature proteins compared with control without preincubation in the absence of GST-AIP. (D) AIP was translated in reticulocyte lysates in the presence of cold methionine. Mock translation without mRNA was also done. After stopping the translation by adding cycloheximide, the AIP- and mock-translated mixtures were combined as indicated (total, 5 μl), and mixed with ^{35}S-labeled human pOTC in 5 μl reticulocyte lysate. The 10-μl mixture was preincubated at 25°C for 20 min in the import reaction mixture without mitochondria (total, 90 μl), and then mixed with isolated mitochondria (total, 100 μl). The import reaction and quantification were done as in A and B. The percentage of import represents the amount of mature proteins compared with control without preincubation in the presence of mock-translated mixture.

gion 126–145 of Tom20. As a result, only one clone encoding full-length AIP was isolated. Specific interaction between AIP and Tom20 was examined (Fig. 1 B). Two nuclear-encoded mitochondrial proteins, enoyl-coenzyme A hydratase 1 precursor (ECHS1; Kanazawa et al., 1993) and NADH:ubiquinone oxidoreductase 1β subcomplex 10 (NDUFB10; Loeffen et al., 1998), which were isolated as proteins interacting with region 101–145 of Tom20, were used as controls. Among AIP, ECHS1, and NDUFB10, only AIP bound to region 126–145 of Tom20, although all bound to region 101–145. Moreover, when four residues (142–145) of the extreme COOH-terminal acidic segment 141–145 (EDDVE) of Tom20 were deleted from the fusions (Fig. 1 A), the binding of AIP to Tom20 was almost completely lost. These results indicate that AIP specifically binds to the extreme COOH-terminal acidic segment of Tom20.

The binding of AIP to Tom20 in vitro was further analyzed (Fig. 1 C). AIP and mitochondrial proteins (pOTC-GFP, ECHS1, and NDUFB10) synthesized in vitro were incubated with glutathione-Sepharose beads prebound with GST, GST-(25–145)hTom20, GST-(25–125)hTom20, or GST-(1–82) Tom22. We reported that the NH_2-terminal portion 1–82 of Tom22 is exposed to the cytosol and binds preproteins (Yano et al., 2000). pOTC-GFP is a fusion protein in which the presequence of pOTC is fused with GFP (Yano et al., 1997). GST fusions and the bound proteins were then eluted with reduced glutathione. Almost 100% of GST fusions that were applied to the binding assay were recovered in the eluate (unpublished data). All mitochondrial proteins tested here bound to all GST fusions (Fig. 1 C), indicating that the mitochondrial proteins bind to both Tom20 and Tom22. The COOH-terminal region 126–145 of Tom20 was dispensable for preprotein binding. In contrast, AIP bound to the entire cytosolic domain of Tom20, but not to the COOH-terminally deleted cytosolic domain, and did not bind to the entire cytosolic domain of Tom22. No protein tested here bound to GST. These results, as well as those from two-hybrid analysis, suggest that AIP binds to the COOH-terminal region of Tom20, which is not required for mitochondrial preprotein binding. In vitro binding assay in the presence of various concentrations of KCl indicated that AIP and Tom20 interact electrostatically (unpublished data).

AIP maintains the import competency of pOTC

When immunoblot analysis was done using anti–human AIP, AIP polypeptides were readily detected in the lysates of HeLa (human), HepG2 (human), COS-7 (monkey), and

Hepa1c1c7 (mouse) cells. The concentration was calculated to be ~0.02–0.1% of total proteins. On the other hand, AIP polypeptide was barely detectable in rabbit reticulocyte lysates (unpublished data). To determine if AIP is involved in mitochondrial protein import, in vitro import of pOTC and pOTC-GFP into mitochondria was examined in the presence of GST-fused AIP (Fig. 2). Both pOTC and pOTC-GFP translated in rabbit reticulocyte lysates are imported into the isolated mitochondria and processed to mature forms (Yano et al., 1997). When the import of pOTC and pOTC-GFP was performed in the presence of 1.0 pmol GST-AIP, the import was little affected. However, it was strongly inhibited by increasing amounts of GST-AIP (Fig. 2 A). The amount of GST-AIP required for 50% inhibition of import of pOTC and pOTC-GFP were ~40 and 150 pmol, respectively (Fig. 2 B). These results indicate that the presequence of pOTC is responsible for the import inhibition by AIP. Thus, the involvement of AIP in mitochondrial protein import was strongly suggested.

It is known that the import competency of pOTC translated in rabbit reticulocyte lysates is lost with time by preincubation without mitochondria. As AIP may have a function to maintain the import competency of pOTC, we preincubated pOTC in the presence of GST-AIP before import into mitochondria (Fig. 2 C). When in vitro–translated pOTC was preincubated at 25°C for 20 min in the absence of GST-AIP, pOTC import was reduced by ~50% compared with control without preincubation. When preincubation was done in the presence of 0.015–1.0 pmol of AIP, the reduction of pOTC import was partially prevented. These results suggest that AIP can maintain the import competency of pOTC. On the contrary, pOTC import was inhibited by increasing the amount of AIP over 4.0 pmol, suggesting that appropriate amounts of AIP are important for positive functions.

Next, we performed similar experiments using the in vitro–translated AIP (Fig. 2 D). The amount of translated AIP in the translation mixture was estimated to be 0.4–2.0 ng (0.01–0.05 pmol)/μl based on immunoblot analysis (unpublished data). When pOTC was preincubated with a mock-translated mixture, the import of pOTC was reduced by ~50%. When preincubation was done in the presence of 1 or 5 μl AIP-translated mixture, the loss of pOTC import was partly prevented. Therefore, the function of AIP to maintain the import competency of pOTC was confirmed.

AIP enhances the import of pOTC

Next, we examined the effect of AIP in cultured cells (Fig. 3). When human pOTC is transiently expressed in COS-7 cells, it is imported into the mitochondria and processed to the mature form, as revealed by cell fractionation and immunoblot analysis (Yano et al., 1997). The plasmids expressing pOTC and GFP (27 kD) were cotransfected with the plasmids expressing EGFP-C1 (EGFP fused with COOH-terminal small tag derived from the multi-cloning site; 30 kD) or EGFP-AIP (EGFP COOH-terminally fused with AIP; 66 kD) in COS-7 cells, and immunoblot analysis of the cell extracts was done (Fig. 3 A). EGFP-C1, EGFP-AIP, and GFP polypeptides were detected using an anti-GFP antibody. There was little difference in expression of GFP, an expression control, in cells overexpressing EGFP-C1 or EGFP-AIP, indicating that transcription and translation were little affected by overexpressed AIP. In contrast, a larger amount of mature ornithine transcarbamylase (OTC) was detected in cells overexpressing EGFP-AIP. The amount of the mature form of pOTC in cells overexpressing EGFP-AIP was about threefold larger than those in cells overexpressing EGFP-C1 (Fig. 3 B). These findings indicate that AIP can enhance the mitochondrial import of pOTC. Endogenous AIP and EGFP-AIP polypeptides were also detected using an anti-AIP antibody. Considering the transfection efficiency (~10–20%), expression of EGFP-AIP in transfected cells was calculated to be ~5–10-fold higher than that of endogenous AIP. Endogenous Hsc70 and glyceraldehyde-3-phosphate dehydrogenase were also immunostained to assess the amounts of applied proteins.

To confirm the function of AIP to enhance the import of pOTC, pulse-chase experiments were conducted. When EGFP-C1 was coexpressed with pOTC, mature OTC and a small amount of unprocessed pOTC were detected after a 20-min pulse, and pOTC disappeared after a 40-min chase (Fig. 3 C). When pOTC was coexpressed with EGFP-AIP instead of EGFP-C1, both unprocessed pOTC and processed mature OTC increased after a pulse by ~2.5-fold (Fig. 3 D). Almost all pOTC disappeared after a chase. When R23GpOTC (a mutant of pOTC that binds to Tom20 but is not transported into the matrix) was coexpressed with EGFP-C1, labeled R23GpOTC was detected after a pulse, and almost all the mutant pOTC disappeared after chase, probably due to cytosolic degradation (Wright et al., 2001). When R23GpOTC was coexpressed with EGFP-AIP, labeled R23GpOTC increased by about threefold after a pulse, and a portion of the mutant pOTC remained after a chase. All these results suggest strongly that AIP stabilizes pOTC in the cytosol and facilitates its import into mitochondria. Synthesis of GFP was little (or not) affected by overexpression of EGFP-AIP, again indicating that in general, AIP does not affect transcription and translation.

Finally, the effect of AIP on preprotein import was examined by depletion experiments using small interfering RNA (siRNA; Fig. 3, E–H). COS-7 cells were cotransfected with synthetic siRNAs and the plasmid expressing pOTC-GFP, and the cell extract was subjected to immunoblot analysis (Fig. 3 E). When control siRNA was cotransfected, a small amount of unprocessed pOTC-GFP and a large amount of processed mature form were detected. In contrast, when siRNA targeted for AIP was cotransfected, the amount of endogenous AIP was reduced to 40% of control, and the amount of unprocessed pOTC-GFP increased markedly. This would indicate that depletion of AIP impairs the mitochondrial import of pOTC-GFP. However, accumulation of the mature form of pOTC-GFP was little affected, probably because depletion of AIP by RNA interference was not complete and because the effect of RNA interference usually appears ~2 d after transfection. Moreover, a stable transformant of HeLa cells expressing siRNA for AIP (HeLa/pSN-AIP) was isolated (Fig. 3, F–H). When the cell extract was subjected to immunoblot analysis, endogenous AIP was reduced to ~30% of control (HeLa/pSN), although expression of Hsc70, GAPDH, mitochondrial porin, and Tom20 was little affected (Fig. 3 F). When HeLa/pSN and HeLa/pSN-AIP were cotransfected with the plasmids expressing pOTC and GFP, the amount of the processed mature form of pOTC in HeLa/pSN-AIP cells was decreased (Fig. 3 G). The amount of

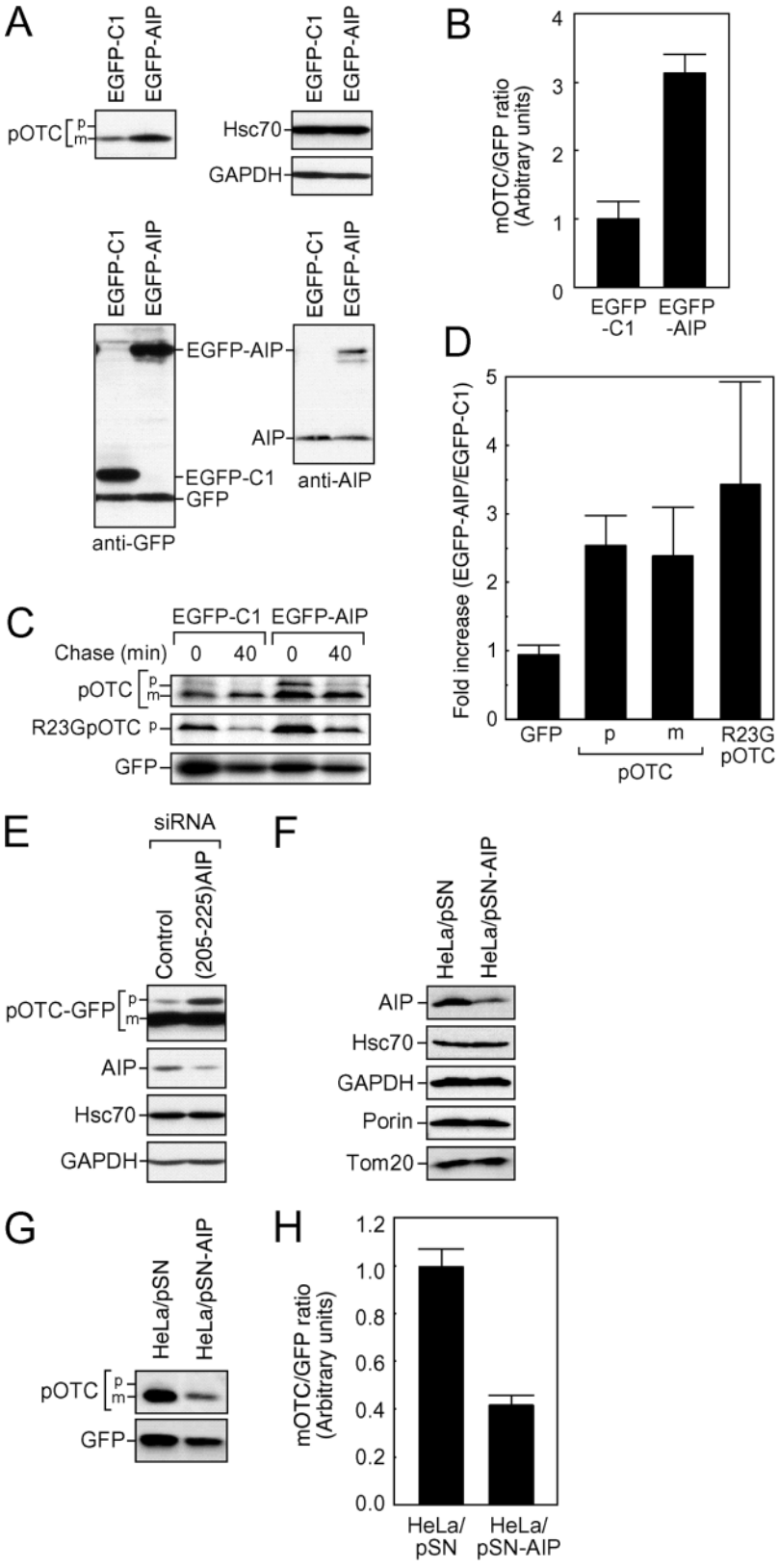

Figure 3. **AIP enhances the import of pOTC in cultured cells.** (A) Both pCAGGS-pOTC (a plasmid expressing pOTC; 5 μg) and pCAGGS-GFP (a plasmid expressing GFP; 5 μg) were cotransfected with pEGFP-C1 (a plasmid expressing EGFP-C1; 5 μg) or pEGFP-AIP (a plasmid expressing EGFP-AIP; 5 μg) into COS-7 cells on 100-mm dishes. After culturing for 36 h, cells were harvested, and the cell extracts (16 μg protein) were subjected to SDS-PAGE and immunoblot analysis for the indicated proteins; p and m, precursor and mature forms, respectively; AIP, endogenous AIP in COS-7; GAPDH, glyceraldehyde-3-phosphate dehydrogenase. (B) GFP and the processed mature OTC (mOTC) in A were quantified. The ratios of mOTC versus GFP were calculated (mean ± SD, $n = 3$). The mean of the values for EGFP-C1–expressing cells was set as 1. (C) 5 μg pCAGGS-pOTC, 5 μg pCAGGS-R23GpOTC (a plasmid expressing R23GpOTC), or 5 μg pCAGGS-GFP were cotransfected with 5 μg pEGFP-C1 or 5 μg pEGFP-AIP into COS-7 cells on 100-mm dishes. After culturing for 36 h, cells were radiolabeled for 20 min and then chased using cold methionine. After a 0- and 40-min chase, proteins were immunoprecipitated with anti-OTC or -GFP antiserum and analyzed by SDS-PAGE and fluorography. (D) The radiolabeled proteins chased for 0 min in C were quantified. The ratios of the indicated radiolabeled proteins in EGFP-AIP–expressing cells (EGFP-AIP) versus those in EGFP-C1–expressing cells (EGFP-C1) are shown as "Fold increase" (mean ± SD, $n = 3$). (E) COS-7 cells on 35-mm dishes were cotransfected with 1 μg pCAGGS-pOTC-GFP and 2.8 μg siRNA. After 3.5 d, the cells were harvested and the cell extract (8 μg protein) was subjected to immunoblot analysis. Control, siRNA for *Discosoma sp.* red fluorescent protein; (205–225)AIP, siRNA for AIP. (F) The extracts (20 μg protein) of HeLa/pSN and HeLa/pSN-AIP cells were subjected to SDS-PAGE and immunoblot analysis for the indicated proteins. (G) HeLa/pSN and HeLa/pSN-AIP cells on 35-mm dishes were cotransfected with 2 μg pCAGGS-pOTC and 2 μg pCAGGS-GFP. After 48 h, the cells were harvested and the cell extract (10 μg protein) was subjected to immunoblot analysis. (H) GFP and mOTC in G were quantified. The ratios of mOTC versus GFP were calculated (mean ± SD, $n = 3$). The mean of the values for HeLa/pSN cells was set as 1.

mature OTC in HeLa/pSN-AIP cells corrected for GFP (an expression control) was ~40% of that in HeLa/pSN cells (Fig. 3 H). Thus, depletion of AIP reduced the mitochondrial import of pOTC, which means that endogenous AIP facilitates pOTC import into mitochondria.

AIP binds to the presequence of pOTC in the same manner as does Tom20

To analyze the interaction between AIP and preproteins, in vitro binding assay was conducted (Fig. 4). Human pOTC and its derivatives synthesized in vitro were incubated with

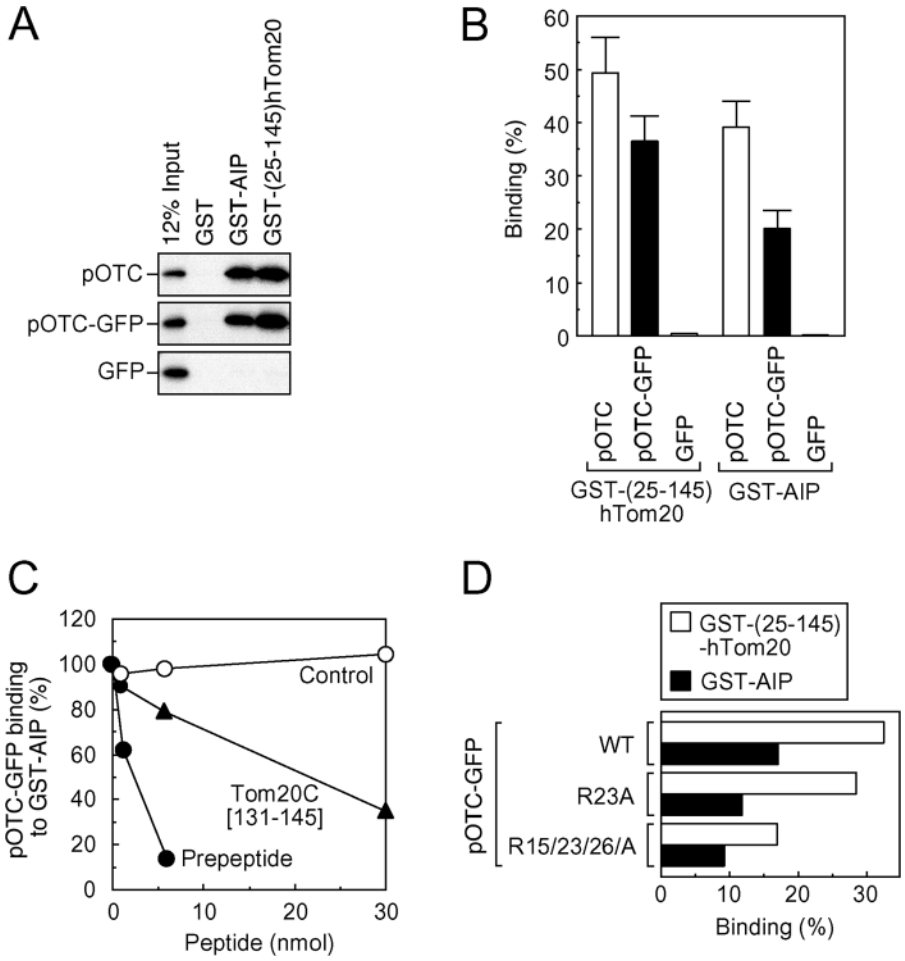

Figure 4. **AIP binds to the presequence peptide of pOTC in the same manner as does Tom20.** (A) Translation mixture containing ^{35}S-labeled pOTC, pOTC-GFP, or GFP (10 μl) was incubated with glutathione-Sepharose beads prebound with GST, GST-AIP, or GST-(25–145)hTom20 (0.6 nmol) in the binding buffer (total, 300 μl). After washing, GST derivatives and bound proteins were eluted and subjected to SDS-PAGE and fluorography. 12% Input: 12% of input ^{35}S-labeled proteins. (B) The radioactive proteins in A were quantified. The binding was expressed as a percentage of input proteins (mean ± SD, $n = 3$). (C) Binding of ^{35}S-labeled pOTC-GFP to GST-AIP (0.6 nmol) was assessed in the binding buffer (total, 300 μl) containing 0, 1.2, 6, and 30 nmol of synthetic presequence peptide of human pOTC (Prepeptide), Tom20C[131–145], or PTH[69–84] (Control) as in A, and quantified as in B. Binding was expressed as a percentage of controls without peptides. (D) Binding of ^{35}S-labeled pOTC-GFP derivatives to GST-AIP or GST-(25–145)hTom20 was assessed and quantified as in A and B. WT, pOTC-GFP; R23A, R23ApOTC-GFP; R15/23/26A, R15/23/26ApOTC-GFP.

glutathione-Sepharose beads prebound with GST-fused AIP or Tom20, and the GST fusions and bound proteins were then eluted (Fig. 4, A and B). About 50% of pOTC and 35% of pOTC-GFP bound to Tom20, whereas no binding of GFP was observed. Therefore, the presequence is critical for preprotein binding to Tom20, as we noted earlier (Yano et al., 2000). When pOTC was subjected to the binding to AIP, ~40% of pOTC and ~20% of pOTC-GFP bound to AIP. These results indicate that AIP (as well as Tom20) binds to pOTC, and that the presequence is important for preprotein binding to AIP.

To confirm the specific binding of AIP to the presequence, effect of synthetic presequence peptide on preprotein binding to AIP was examined (Fig. 4 C). The binding of pOTC-GFP to AIP decreased markedly with increasing concentrations of the presequence peptide, whereas the control peptide did not affect the binding. These results indicate that the presequence is critical for AIP binding to pOTC-GFP. Furthermore, when a synthetic peptide corresponding to region 131–145 of Tom20 (Tom20C[131–145]) was added, the binding decreased gradually with increasing concentrations of Tom20C[131–145], thereby indicating that in AIP, the presequence-binding site is close to the Tom20-binding site.

Next, we determined if AIP and Tom20 interact with the presequence in the same manner (Fig. 4 D). When pOTC-GFP mutants R23A and R15/23/26A, in which one (position 23) or three (positions 15, 23, and 26) Arg residues in the presequence of pOTC-GFP were replaced by Ala, were used for in vitro binding assay, preprotein binding to AIP as well as to Tom20 decreased in a stepwise way as the number of replacements increased. These results indicate that positive charges in the presequence are important for binding to AIP as well as to Tom20. However, the triple mutant still showed moderate binding. Hydrophobic interaction appears to be important for AIP binding to the presequence, as noted for the Tom20-presequence binding (Abe et al., 2000; Yano et al., 2000). The in vitro binding assay of pOTC-GFP in the presence of KCl and Triton X-100 also indicated that binding of the presequence to AIP as well as to Tom20 is mediated mainly by hydrophobic interactions (unpublished data).

AIP binds specifically to mitochondrial preproteins

To confirm the specific interaction between AIP and mitochondrial preproteins, we performed the binding assays using various mitochondrial and nonmitochondrial proteins (Fig. 5). When mitochondrial preproteins with typical NH_2-terminal presequences, including ECHS1, preaspartate aminotransferase (pAAT), and preserine:pyruvate aminotransferase (pSPT) were used, they bound to AIP as well as to Tom20. The fusion proteins pAAT-GFP and pSPT-GFP, in which the presequences of pAAT and pSPT, respectively, were fused to GFP, also bound to AIP as well as to Tom20. Hence, AIP can recognize various presequences of mitochondrial preproteins. In addition, other mitochondrial pre-

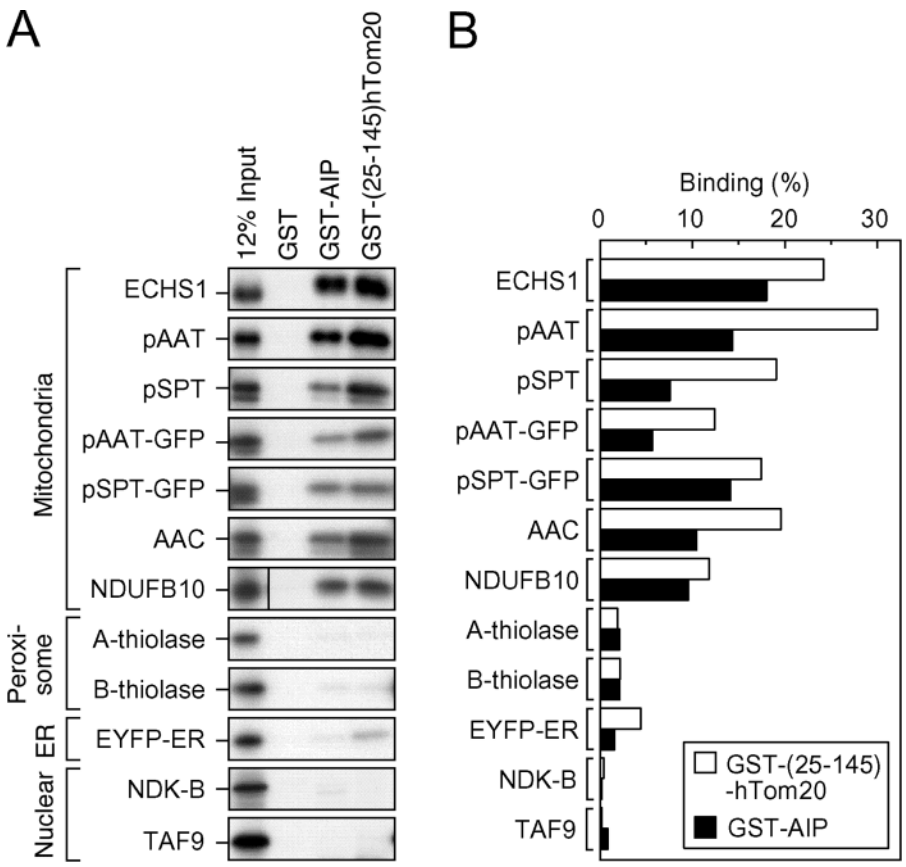

Figure 5. **AIP and Tom20 bind to mitochondrial preproteins in a similar manner.** (A) Binding of various ^{35}S-labeled mitochondrial and nonmitochondrial proteins to GST-AIP or GST-(25–145)-hTom20 was assessed and quantified. pAAT, preaspartate aminotransferase; pSPT, preserine:pyruvate aminotransferase; AAC, ATP/ADP carrier protein; EYFP-ER, EYFP fused with ER targeting and retrieval signals of calreticulin; NDK-B, nucleoside diphosphate kinase B; TAF9, TATA-binding protein–associated factor. (B) The radioactive proteins in A were quantified. The binding is expressed as a percentage of the input proteins.

proteins, ATP/ADP carrier protein and NDUFB10, which lack a cleavable presequence, also bound to AIP as well as to Tom20. These results strongly suggest that AIP recognizes not only typical presequences, but also internal import signals of mitochondrial preproteins. Furthermore, AIP and Tom20 appeared to have a similar binding preference to each different preprotein, although AIP bound to preproteins less strongly than did Tom20. In contrast, no or little binding of AIP and Tom20 to proteins destined for other organelles, including peroxisomes, ER, and nucleus, was observed. These results indicate that AIP as well as Tom20 binds specifically to mitochondrial preproteins.

AIP has a chaperone-like activity to suppress thermal aggregation of proteins

FKBP52 was reported to have chaperone-like activity (Bose et al., 1996; Pirkl et al., 2001) and prevented thermal aggregation of the model substrates rhodanese and citrate synthase in vitro. As AIP has a significant homology with FKBP52, we asked whether AIP also has chaperone-like activity to suppress aggregation of mitochondrial preproteins. First, we examined the effect of AIP on rhodanese. When aggregation of rhodanese was monitored by light scattering at 55°C, rhodanese began to aggregate after 1 min, and reached a plateau at ~10 min (Fig. 6 A). The addition of equal amounts of GST did not affect the pattern of aggregation, although a larger number of aggregates was formed. This increased aggregation was attributable to thermal aggregation of GST itself (Fig. 6 C). On the contrary, when GST-AIP was added instead of GST, the aggregation was suppressed at early time points, showing that AIP has chaperone-like activity to suppress the thermal aggregation of rhodanese. The higher aggregation seen at later time points was apparently due to the aggregation of GST-AIP (Fig. 6 C).

Also, we monitored the effect of AIP on citrate synthase. Upon incubation at 43°C, the aggregation of citrate synthase began after 4 min, and reached the maximum at ~15 min (Fig. 6 B). The pattern of aggregation was not influenced whenever a 10-fold larger amount of GST was added; yet when an equal amount of GST-AIP was added, the aggregation of citrate synthase was suppressed. Addition of GST-AIP in a 3.3-fold excess led to much stronger suppression of aggregation.

The aggregated proteins were then analyzed using SDS-PAGE (Fig. 6 C). When rhodanese or citrate synthase was incubated with GST, aggregation of the tested proteins occurred. In contrast, when GST-AIP was added instead of GST, the aggregation of rhodanese was partially suppressed, and that of citrate synthase was completely suppressed. These results reconfirmed that AIP has chaperone-like activity. Thus, AIP appears to bind to unfolded proteins in addition to the presequence of mitochondrial preproteins. This chaperone-like activity may be important to maintain mitochondria-targeted preproteins unfolded and to suppress their aggregation in the cytosol.

Because Hsc70 (as well as AIP) is involved in the process of AhR complex maturation, it is possible that AIP and Hsc70 cooperate to suppress the protein aggregation. Therefore, we examined the effect of AIP on citrate synthase in the presence of Hsc70 (Fig. 6 D). Although the aggregation was suppressed in the presence of 0.15 μM Hsc70, the combination of 0.15 μM AIP and 0.15 μM Hsc70 suppressed the

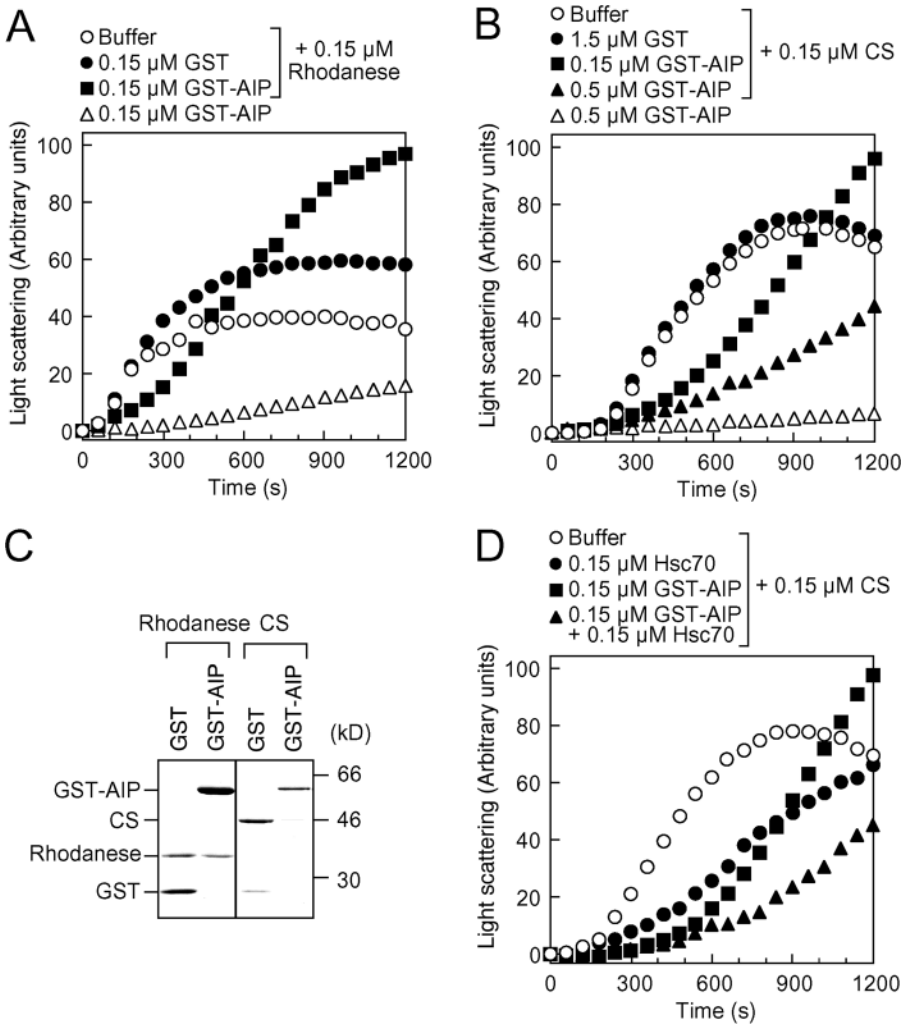

Figure 6. **AIP has a chaperone-like activity.** (A) Aggregation of 0.15 μM rhodanese was monitored at 55°C in the absence (Buffer) or presence of indicated mounts of GST fusions by measuring the turbidity of the solution at 360 nm. (B) Aggregation of 0.15 μM citrate synthase (CS) was monitored at 43°C as in A. (C) Aggregation of 0.15 μM rhodanese and 0.15 μM citrate synthase was done in the presence of 0.5 μM GST or 0.5 μM GST-AIP. Aggregation of rhodanese was tested at 55°C for 4 min, and that of citrate synthase was tested at 43°C for 10 min. Aggregated proteins were recovered by centrifugation, subjected to SDS-PAGE, and stained with Coomassie brilliant blue R-250. (D) Aggregation of 0.15 μM citrate synthase was monitored in the solution containing 1 mM ATP-$MgCl_2$ at 43°C.

aggregation more efficiently, hence, the effects of Hsc70 and AIP are additive or synergistic.

Preprotein forms a ternary complex with AIP and Tom20

As mitochondria-targeted preproteins synthesized in cytosol are transferred to the mitochondrial import receptors at the initial step of import, we considered that preproteins complexed with AIP are transferred to Tom20 and that a ternary complex is formed. To check this possibility, we asked if the complex formation between preprotein and AIP would be influenced by addition of the cytosolic domain of Tom20 (Fig. 7, A and B). In vitro–translated pOTC-GFP was incubated with GST-AIP bound to glutathione-Sepharose beads in the presence of maltose-binding protein (MBP) fused with LacZ (MBP-LacZ), the cytosolic domain of Tom20 (MBP-cT20), or AIP (MBP-AIP). Bound proteins to GST-AIP were then eluted with glutathione. MBP-LacZ did not affect the binding of pOTC-GFP to GST-AIP. When MBP-AIP was added, the binding of pOTC-GFP to GST-AIP was reduced by ~50%, probably due to competition (Fig. 7 B). On the other hand, when MBP-cT20 was added, binding of MBP-cT20 to GST-AIP occurred, thereby indicating the complex formation between MBP-cT20 and GST-AIP. The bound pOTC-GFP increased by 1.5-fold, indicating that MBP-cT20 complexed with GST-AIP also contains pOTC-GFP. These results suggest that pOTC-GFP, AIP, and Tom20 form a ternary complex. We also performed binding assays using MBP-cT20 bound to amylose beads in the presence of GST or GST-AIP. Proteins bound to MBP-cT20 were eluted with maltose. When GST-AIP was added instead of GST, a complex formation between GST-AIP and MBP-cT20 was observed. The amount of bound pOTC-GFP increased by ~1.4-fold. Thus, the ternary complex formation among pOTC-GFP, AIP, and Tom20 was confirmed.

It has been reported that many mitochondrial preproteins synthesized in the cytosol are complexed with chaperones such as Hsc70 (Komiya et al., 1996, 1997; Terada et al., 1996; Artigues et al., 2002; Hoogenraad et al., 2002). To determine if Hsc70 is also involved in a complex formation with AIP, binding assays were conducted (Fig. 7 C). pOTC-GFP was confirmed to bind to AIP (lane 6) and Tom20 (lane 8), respectively. Hsc70 was found to bind to AIP in the presence of pOTC-GFP (lane 6), and this binding was little affected in the absence of pOTC-GFP (lane 5). In contrast, the binding of Hsc70 to Tom20 was not observed (lane 7 and lane 8). Hsp70 was reported to dissociate from preprotein when the preprotein–Hsp70 complex is transferred to Tom20 (Komiya et al., 1997). Little binding was observed between AIP and Hsp90 (lane 5 and lane 6), and no binding was observed between Tom20 and Hsp90 (lane 7 and lane 8). It was also re-

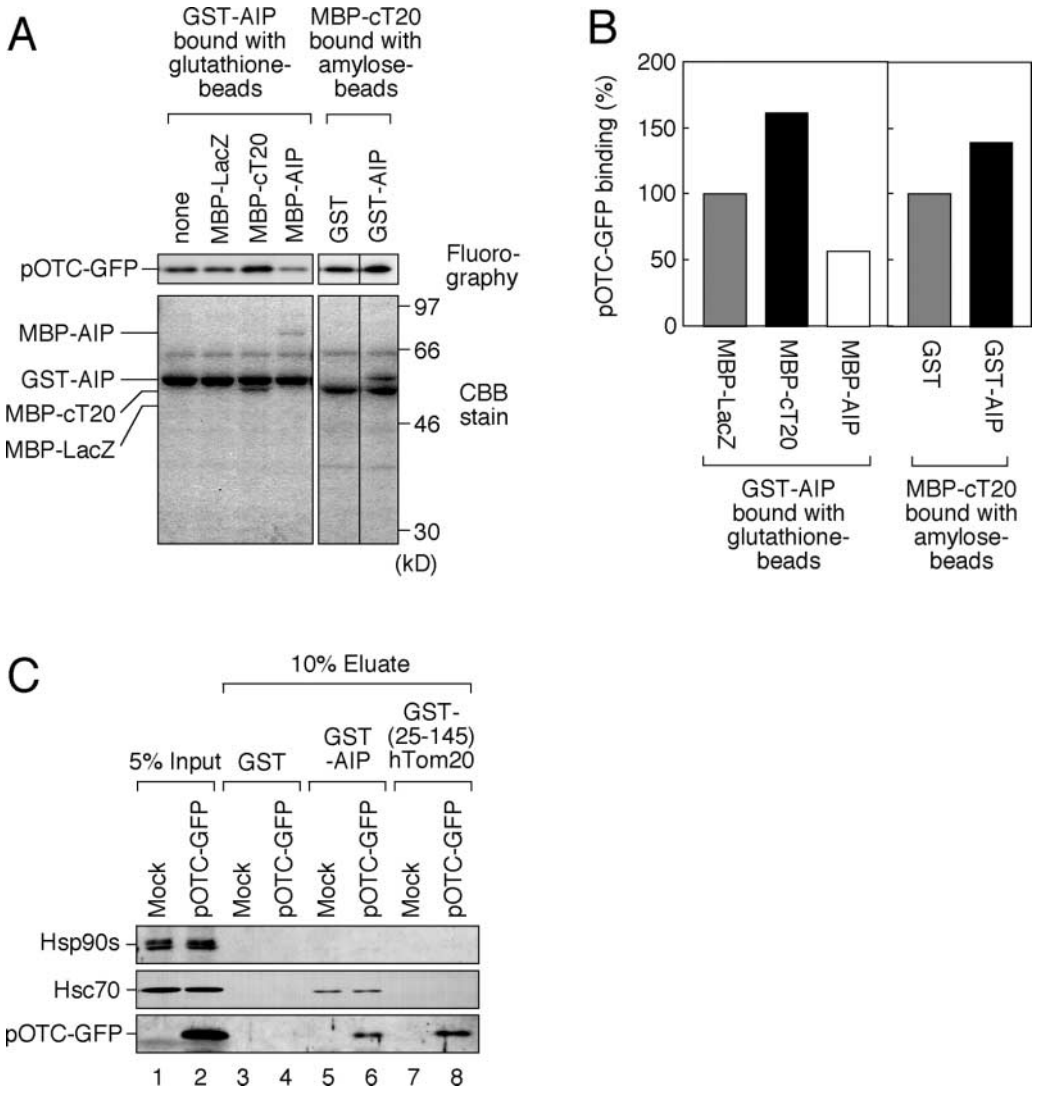

Figure 7. **Complex formation among preprotein, AIP, Tom20, and other chaperones.** (A) Ternary complex formation of preprotein, AIP, and Tom20 was examined. The translation mixture containing 10 μl ^{35}S-labeled pOTC-GFP was incubated with GST or MBP derivatives (0.2 nmol) bound to glutathione beads or amylose beads in the presence of purified MBP or GST derivatives (0.2 nmol). After washing, GST and MBP derivatives with bound proteins were eluted and subjected to SDS-PAGE, followed by staining with Coomassie brilliant blue R-250 (CBB) and fluorography. (B) The radioactive preproteins in A were quantified. The binding is expressed as percentage of controls with MBP-LacZ or GST. (C) The involvement of Hsc70 and Hsp90s in preprotein binding to AIP was examined. The translation mixture containing 10 μl nonlabeled pOTC-GFP was subjected to a binding assay, as in Fig. 4 A. The eluate was subjected to SDS-PAGE followed by immunoblot analysis.

ported that AIP does not bind to Hsp90 in rabbit reticulocyte lysates, which do not contain AhR (Meyer et al., 1998). These results indicate that AIP preferentially forms a complex with Hsc70 rather than with Hsp90 in the absence of AhR.

TPR motifs of AIP are responsible for interactions with Tom20, whereas both a small PPIase domain and TPR motifs are required for interaction with preproteins

Finally, we did two-hybrid assays to determine the region on AIP responsible for binding to Tom20 and preproteins (Fig. 8). A series of AIP mutants were constructed as fusion proteins with B42AD or LexA (Fig. 8 A). The entire AIP fused with LexA, but not other mutant AIP fusions, had a self-activating phenotype.

The interaction between Tom20 and AIP mutants was first examined (Fig. 8 B). As shown in Fig. 1, full-length AIP bound to regions 101–145 and 126–145 of Tom20, but not to regions 101–141 and 126–141, thus confirming that the extreme COOH-terminal acidic segment of Tom20 is responsible for binding to AIP. Furthermore, two AIP deletion mutants harboring region 96–330 and 172–330 also bound to Tom20. As TPR motifs are commonly included in these two regions, the TPR motifs in AIP are suggested to be responsible for the binding with Tom20.

Next, interactions between AIP mutants and preproteins were examined (Fig. 8 C). One AIP mutant harboring region 96–330 bound to preproteins. Region 96–330 of AIP contains a small PPIase domain and TPR motifs. However, neither region 96–171 nor region 172–330 of AIP alone bound to preproteins. These results suggest that both region 96–171 and the following TPR motifs are responsible for preprotein binding.

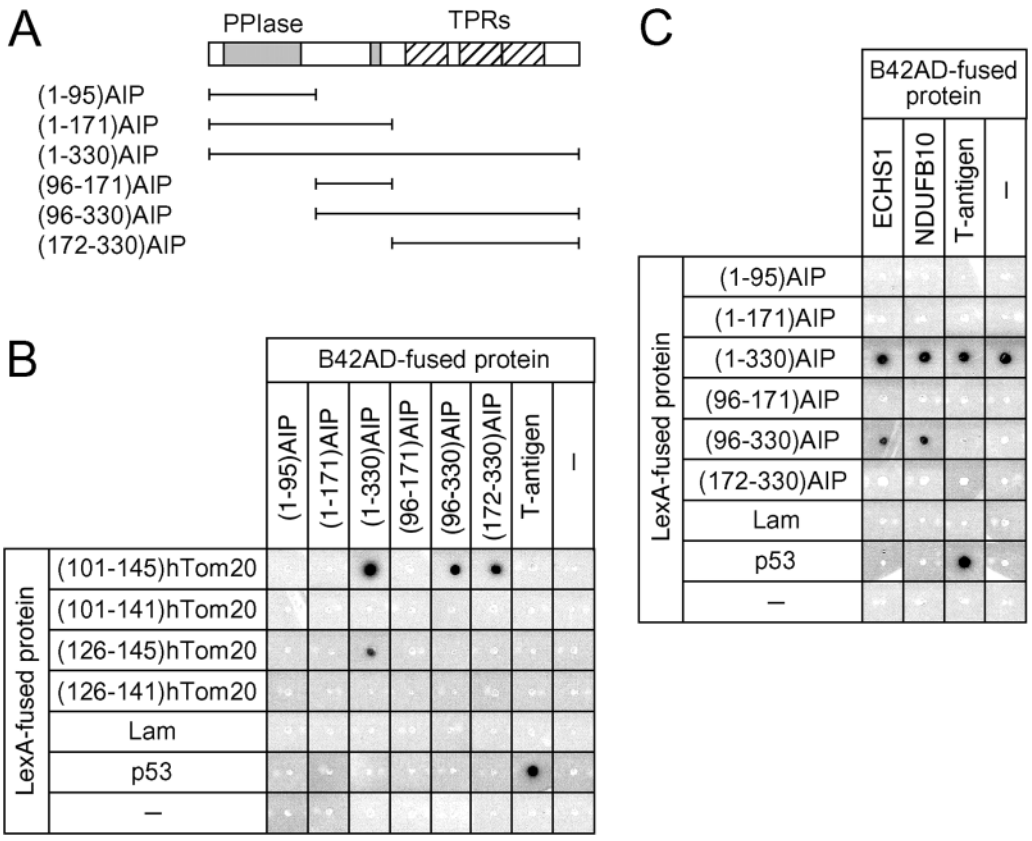

Figure 8. **Two-hybrid analysis of the binding sites for Tom20 and preproteins in AIP.** (A) The schematic structures of AIP and its deletion mutants fused with LexA are shown. PPIase, a domain homologous to that of peptidyl-prolyl cis/trans isomerase; TPRs, three tetratricopeptide-repeat motifs. (B and C) Interaction between LexA-fused hTom20s and B42AD-fused AIPs (B) and interaction between LexA-fused AIPs and B42AD-fused mitochondrial preproteins (C) were analyzed as in Fig. 1 B.

Discussion

In the present work, we identified AIP to be a Tom20-interacting protein by stepwise screening using a two-hybrid system (Fig. 1). Further experiments using a two-hybrid analysis and an in vitro binding assay revealed that the extreme COOH-terminal acidic segment (in human, EDDVE) of Tom20 interacts with TPR motifs in AIP (Fig. 1 and Fig. 8).

Involvement of AIP in mitochondrial preprotein import was first suggested by the finding that an excess amount of AIP inhibited the import of pOTC and pOTC-GFP into isolated mitochondria (Fig. 2). However, the observed inhibition may be attributable to the relative insufficiency in rabbit reticulocyte lysates of other import factors that collaborate with AIP. Indeed, we found that the smaller amounts of AIP can maintain the import competency of pOTC. Overexpression of AIP in cultured cells resulted in enhancement of pOTC import (Fig. 3). Overexpressed AIP stabilized pOTC derivatives in the cytosol in 20-min pulse experiments. However, overexpressed AIP seemed to have little effect on preventing preproteins from cytosolic degradation in a 40-min chase. The possible explanation is that AIP prevents preproteins from degradation only until the preproteins are transferred to the mitochondrial receptor Tom20. As pOTC-GFP is more stable in the cytosol than is pOTC (Yano et al., 1998), we could show that pOTC-GFP import is impaired by depletion of AIP. In addition, by using a stable transformant of HeLa cells expressing siRNA, we showed that import of pOTC is decreased by depletion of AIP. Thus, it was confirmed that endogenous AIP stabilizes pOTC in the cytosol and facilitates its import into mitochondria.

An in vitro binding assay indicated that AIP binds to the presequence of pOTC, and that the presequence-binding site of AIP is close to that for the COOH-terminal segment of Tom20 (Fig. 4). These observations further suggest that AIP is involved in the import pathway in which preproteins are targeted directly to Tom20. Actually, formation of a ternary complex of preprotein, AIP, and Tom20 was observed (Fig. 7). AIP and Tom20 appear to bind to the presequence of pOTC in a similar manner (Fig. 4). Specific interaction between AIP and other mitochondrial preproteins was also observed (Fig. 5). AIP was found to function as a chaperone to suppress thermal aggregation of rhodanese and citrate synthase (Fig. 6). AIP may function as a chaperone to maintain mitochondria-targeted preproteins unfolded and to suppress their aggregation. Furthermore, Hsc70 appears to cooperate with AIP for this chaperone-like activity. In fact, Hsc70 was also found to bind to AIP (Fig. 7). As the COOH-terminal acidic residues (EEVD) of Hsc70 resembles that of Tom20 (EDDVE), the COOH-terminal segment of Hsc70 may also bind to TPR motifs in AIP. We consider that the preprotein–Hsc70 complex forms a larger complex with AIP in the cytosol. Together with Hsc70, the chaperone-like activity of AIP may also function to maintain preproteins in an unfolded state. When the complex is transferred to the mitochondria, it may form a complex with

Tom20. As AIP apparently binds to preprotein less strongly than does Tom20, the preprotein may be transferred to Tom20 from AIP. The present results will much advance our understanding of molecular mechanism of Tom20-dependent targeting of preproteins from the cytosol to the mitochondria.

Materials and methods

Peptides

PTH[69–84] peptide (EADKADVNVLTKAKSQ) corresponding to the region 69–84 of human parathyroid hormone was purchased from Peptide Institute, Inc. Tom20C[131–145] peptide (QRIVSAQSLAEDDVE) corresponding to the COOH-terminal portion of hTom20 and the presequence peptide (MLFNLRILLNNAAFRNGHNFMVRNFRCGQPLQ) corresponding to the presequence of human pOTC was commercially synthesized.

Plasmids

To construct plasmids expressing LexA-fused proteins and B42AD-fused proteins for two-hybrid assays, pLexA and pB42AD plasmids (CLONTECH Laboratories, Inc.) were used. The pB42AD derivatives encoding B42AD-fused proteins with AIP, ECHS1, and NDUFB10 were isolated from positive clones identified by two-hybrid screening. To construct the plasmids for in vitro transcription, cDNA fragments were cloned into pGEM3Zf(+) (Promega). The resulting plasmids, pGEM3Zf(+)-AIP, pGEM3Zf(+)-ECHS1, pGEM3Zf(+)-NDUFB10, pGEM3Zf(+)-NDK-B, and pGEM3Zf(+)-TAF9 express mRNAs for AIP, ECHS1, NDUFB10, NDK-B, and TAF9, respectively. Also, the resulting plasmids pGEM3Zf(+)-pAAT-GFP and pGEM3Zf(+)-pSPT-GFP express mRNAs for pAAT-GFP and pSPT-GFP in which the presequences of pAAT (29 aa) and pSPT (22 aa), respectively, were fused with GFP. To construct pGEM3Zf(+)-EYFP-ER, the EYFP-ER gene was excised from pEYFP-ER (CLONTECH Laboratories, Inc.) and cloned into pGEM3Zf(+). The plasmid pcDNA3.1/GS harboring ATP/ADP carrier was purchased from Invitrogen. To construct pEGFP-AIP expressing EGFP-AIP, the cDNA fragment for AIP was excised from pGEM3Zf(+)-AIP and cloned into pEGFP-C1 (CLONTECH Laboratories, Inc.). To construct pCAGGS-R23GpOTC expressing R23GpOTC, the gene coding R23GpOTC was excised from pGEM3Zf(+)-R23GpOTC (Yano et al., 1997) and cloned into pCAGGS (Niwa et al., 1991). To construct the plasmids pGEX-2T-AIP expressing GST-AIP and pMAL-c2-AIP expressing MBP-AIP, the cDNA fragment for AIP was cloned into pGEX-2T (Amersham Biosciences) and pMAL-c2 (New England Biolabs), respectively. To construct the plasmid pMAL-c2-cT20 expressing MBP-cT20, the gene coding the cytosolic domain of hTom20 (region 25–145) was cloned into pMAL-c2. Construction of pGEM3Zf(+)-pOTC, pGEM3Zf(+)-pOTC-GFP, pGEM3Zf(+)-R23ApOTC-GFP, pGEM3Zf(+)-R15/23/26ApOTC-GFP, pGEX-2T-(25–145)hTom20, pGEX-2T-(25–125)hTom20, pGEX-2T-(1–82)hTom22, pCAGGS-pOTC, pCAGGS-GFP, and pCAGGS-pOTC-GFP was as described previously (Yano et al., 1997, 1998, 2000).

Yeast two-hybrid analysis

The MATCHMAKER™ LexA Two-Hybrid System (CLONTECH Laboratories, Inc.) was used to screen proteins that interact with the COOH-terminal portion of Tom20. Yeast EGY48 containing a lacZ reporter gene (EGY48[p8op-lacZ]) were cotransformed with pLexA-(101–145)hTom20 and human fetal liver pB42AD library plasmids (CLONTECH Laboratories, Inc.). Screening was done according to the manufacturer's instructions. To confirm the specific interaction, each pB42AD derivative was cotransformed with pLexA derivatives in EGY48[p8op-lacZ] and cultured at 30°C for 2 d to amplify the plasmids. The yeast cells were then spotted onto an indicator medium plate, grown at 30°C for 2 d, and checked for development of a blue color.

Protein expression and purification

The plasmids encoding GST- or MBP-fused proteins were transformed into TOPP2 cells (Stratagene). Expression and purification of GST-fused proteins were done as described previously (Yano et al., 1998). MBP-fused proteins were expressed and purified using amylose resin (New England Biolabs) according to the manufacturer's protocol.

Antibodies

The purified GST-AIP protein was used for raising anti-AIP antibodies in a rabbit. Anti-AIP antibodies were affinity purified using *N*-hydroxysuccinimide–activated Sepharose HP (Amersham Biosciences) conjugated with His_6-AIP. Anti–human Hsc70 and Hsp90 antibodies were purchased from Santa Cruz Biotechnology, Inc. Anti–human glyceraldehyde-3-phosphate dehydrogenase antibody was purchased from CHEMICON International. Anti-porin antibody was purchased from Calbiochem-Novabiochem. Anti–human OTC, anti–human Tom20, and anti-GFP antiserum were prepared as described previously (Yano et al., 1998).

In vitro transcription and translation

mRNAs for human AIP, ECHS1, NDUFB10, pOTC, ATP/ADP carrier protein, NDK-B, TAF9, pig pAAT (Nishi et al., 1989), rat pSPT (Oda et al., 1990), A- and B-thiolase (Tsukamoto et al., 1994), pOTC-GFP, R23ApOTC-GFP, R15/23/26ApOTC-GFP, GFP, pAAT-GFP, and pSPT-GFP were synthesized by in vitro transcription. In vitro translation for these RNA transcripts was done as described previously (Yano et al., 2000). Translation was stopped by adding 50 μg/ml cycloheximide.

In vitro binding assay

Purified GST-fused proteins were absorbed onto glutathione-Sepharose beads in binding buffer (20 mM Hepes-KOH, pH 7.4, 50 mM KCl, 1 mM $MgCl_2$, and 0.1 mg/ml BSA). The beads were washed three times in the same buffer. The suspension of beads bound with GST derivatives was withdrawn and mixed with 10 μl of a reticulocyte lysate containing ^{35}S-labeled proteins in the binding buffer (total 300 μl) for 30 min at 25°C with gentle shaking. Unbound proteins were removed by centrifugation in a centrifugal filter unit (Ultrafree-MC; Millipore), and the retained beads were washed once with binding buffer. Bound proteins were eluted by adding elution buffer A (50 mM Tris-HCl, pH 8.0, and 15 mM glutathione), and the eluate was subjected to SDS-PAGE. Radioactivity in the gels was visualized and quantified using an image plate analyzer (FUJIX BAS2000; Fuji Film Co.). Elution of proteins was checked by staining the proteins with Coomassie brilliant blue R-250. When MBP-fused proteins were used, they were absorbed onto amylose beads. Binding and washing were done using the same binding buffer used for GST-fused proteins. Bound proteins were eluted by adding elution buffer B (20 mM Tris-HCl, pH 8.0, 20 mM maltose, 200 mM NaCl, and 1 mM EDTA).

In vitro import into isolated mitochondria

Isolation of HeLa cell mitochondria was done as described previously (Yano et al., 2000). The reticulocyte lysate containing ^{35}S-labeled preproteins was incubated with purified GST-fused proteins or the reticulocyte lysate containing in vitro–translated proteins. When preincubation was done, the mixture was incubated for 20 min at 25°C before the import reaction. Isolated mitochondria (25 μg protein) were added into the mixture and incubated for 20 min at 25°C to allow for the import reaction. The import reaction was stopped by adding 0.1 mM dinitrophenol, and mitochondria were reisolated by centrifugation.

Cell culture and transfection

COS-7 and HeLa cells were cultured in DME with 10% FCS at 37°C in an atmosphere of 5% CO_2 and 95% air. G418-resistant transformants were cultured in the presence of 800 μg/ml G418 (Life Technologies). Transfection was performed using TransIT LT1 polyamine (PanVera Corp.) or LipofectAMINE™ 2000 (Invitrogen).

Immunoblot analysis of cell extracts

Proteins were extracted from cultured cells with PBS containing 1% Triton X-100. The extracted proteins were subjected to SDS-PAGE and immunoblot analysis. Immunodetection was done using ECL kits (Amersham Biosciences). Chemiluminescence signals were detected and quantified using a bioimage analyzer (Las-1000 Plus; Fuji Film Co.).

Pulse-chase experiments

COS-7 cells transfected with plasmids were harvested with trypsinization, washed twice with methionine-free DME, and suspended in 1 ml of the same medium. The cell suspension was incubated at 37°C for 1 h to deplete methionine. The cells were then radiolabeled with 8 Megabecquerels (MBq) of Pro-Mix containing L-[^{35}S]methionine and L-[^{35}S]cysteine for 20 min, and were then chased with 20 mM L-methionine in 2 ml DME. After 0 and 40 min, 0.5-ml aliquots were withdrawn and mixed with 0.5 ml of ice-cold lysis buffer (20 mM Tris-HCl, pH 7.4, 4 mM EDTA, 0.2% SDS, 0.2% Triton X-100, 100 μM chymostatin, 100 μM pepstatin, 100 μM leupeptin, and 100 μM antipain). Proteins were immunoprecipitated with 20 μl antisera and 200 μl of a 10% suspension of protein A–Sepharose.

RNA interference

The double-stranded siRNA 21-mer oligos for AIP were designed for the sequence corresponding to bases 205–225 of human AIP. The control siRNA corresponds to bases 136–156 of *Discosoma sp.* red fluorescent protein.

To construct stable transformants expressing siRNA, siRNA oligonucleotides that contained a sense strand of 19 nucleotide sequences corresponding to bases 531–549 of human AIP followed by a short spacer (GAGTACTG), the reverse complement of the sense strand, and five thymidines as an RNA polymerase III transcriptional stop signal were designed. Forward and reverse oligos were 5′-TCGAGGGCAGTGCCACTTATCCACGAGTACTGGTGGATAAGTGGCACTGCCTTTTT-3′ and 5′-CTAGAAAAAGGCAGTGCCACTTATCCACCAGTACTCGTGGATAAGTGGCACTGCCC-3′. The oligos were annealed and cloned into the SalI/XbaI site of pSuppressorNeo (pSN; Imgenex) to give pSN-AIP. pSN and pSN-AIP were introduced into HeLa cells using LipofectAMINE™ 2000, and G418-resistant transformants were selected in growth medium containing 800 μg/ml G418. From the transformants, a pSN-transformed clone (designated as HeLa/pSN) and a pSN-AIP–transformed clone (designated as HeLa/pSN-AIP) were purified by limited dilution.

Chaperone assay

Thermal denaturation of rhodanese (0.15 μM) was achieved by incubation at 55°C in 40 mM sodium phosphate buffer (pH 7.4), and that of citrate synthase (0.15 μM) was done by incubation at 43°C in 40 mM Hepes-KOH, pH 7.5 (Pirkl et al., 2001). Aggregation was measured by light scattering in a fluorescence spectrophotometer (model F4500; Hitachi) equipped with a thermostated cell holder at an excitation and emission wavelength of 360 nm. Rhodanese and citrate synthase were purchased from Sigma-Aldrich.

We thank J. Miyazaki (Osaka University, Osaka, Japan) for pCAGGS; T. Osumi (Himeji Institute of Technology, Himeji, Japan) for plasmids expressing A- and B-thiolase; and colleagues of the Mori laboratory for discussions. Language assistance was provided by M. Ohara.

This work was supported by grants-in-aid 12780541 and 14780550 (to M. Yano), and 10557020 (to M. Mori) from the Ministry of Education, Science, Technology, Sports and Culture of Japan.

Submitted: 12 May 2003
Accepted: 25 August 2003

References

Abe, Y., T. Shodai, T. Muto, K. Mihara, H. Torii, S. Nishikawa, T. Endo, and D. Kohda. 2000. Structural basis of presequence recognition by the mitochondrial protein import receptor Tom20. *Cell.* 100:551–560.

Artigues, A., A. Iriarte, and M. Martinez-Carrion. 2002. Binding to chaperones allows import of a purified mitochondrial precursor into mitochondria. *J. Biol. Chem.* 277:25047–25055.

Bell, D.R., and A. Poland. 2000. Binding of aryl hydrocarbon receptor (AhR) to AhR-interacting protein. The role of hsp90. *J. Biol. Chem.* 275:36407–36414.

Bose, S., T. Weikl, H. Bugl, and J. Buchner. 1996. Chaperone function of Hsp90-associated proteins. *Science.* 274:1715–1717.

Carver, L.A., and C.A. Bradfield. 1997. Ligand-dependent interaction of the aryl hydrocarbon receptor with a novel immunophilin homolog *in vivo*. *J. Biol. Chem.* 272:11452–11456.

Galat, A., and S.M. Metcalfe. 1995. Peptidylproline *cis/trans* isomerases. *Prog. Biophys. Mol. Biol.* 63:67–118.

Gautschi, M., H. Lilie, U. Funfschilling, A. Mun, S. Ross, T. Lithgow, P. Rucknagel, and S. Rospert. 2001. RAC, a stable ribosome-associated complex in yeast formed by the DnaK-DnaJ homologs Ssz1p and zuotin. *Proc. Natl. Acad. Sci. USA.* 98:3762–3767.

Gautschi, M., A. Mun, S. Ross, and S. Rospert. 2002. A functional chaperone triad on the yeast ribosome. *Proc. Natl. Acad. Sci. USA.* 99:4209–4214.

Goebl, M., and M. Yanagida. 1991. The TPR snap helix: a novel protein repeat motif from mitosis to transcription. *Trends Biochem. Sci.* 16:173–177.

Goping, I.S., D.G. Millar, and G.C. Shore. 1995. Identification of the human mitochondrial protein import receptor, huMas20p. *FEBS Lett.* 373:45–50.

Herrmann, J.M., and W. Neupert. 2000. Protein transport into mitochondria. *Curr. Opin. Microbiol.* 3:210–214.

Hoogenraad, N.J., L.A. Ward, and M.T. Ryan. 2002. Import and assembly of proteins into mitochondria of mammalian cells. *Biochim. Biophys. Acta.* 1592: 97–105.

Kanazawa, M., A. Ohtake, H. Abe, S. Yamamoto, Y. Satoh, M. Takayanagi, H. Niimi, M. Mori, and T. Hashimoto. 1993. Molecular cloning and sequence analysis of the cDNA for human mitochondrial short-chain enoyl-CoA hydratase. *Enzyme Protein.* 47:9–13.

Komiya, T., M. Sakaguchi, and K. Mihara. 1996. Cytoplasmic chaperones determine the targeting pathway of precursor proteins to mitochondria. *EMBO J.* 15:399–407.

Komiya, T., S. Rospert, G. Schatz, and K. Mihara. 1997. Binding of mitochondrial precursor proteins to the cytoplasmic domains of the import receptors Tom70 and Tom20 is determined by cytoplasmic chaperones. *EMBO J.* 16: 4267–4275.

Lang, K., F.X. Schmid, and G. Fischer. 1987. Catalysis of protein folding by prolyl isomerase. *Nature.* 329:268–270.

Lill, R., F.E. Nargang, and W. Neupert. 1996. Biogenesis of mitochondrial proteins. *Curr. Opin. Cell Biol.* 8:505–512.

Lithgow, T., B.S. Glick, and G. Schatz. 1995. The protein import receptor of mitochondria. *Trends Biochem. Sci.* 20:98–101.

Loeffen, J.L., R.H. Triepels, L.P. van den Heuvel, M. Schuelke, C.A. Buskens, R.J. Smeets, J.M. Trijbels, and J.A. Smeitink. 1998. cDNA of eight nuclear encoded subunits of NADH:ubiquinone oxidoreductase: human complex I cDNA characterization completed. *Biochem. Biophys. Res. Commun.* 253:415–422.

Ma, Q., and J.P. Whitlock, Jr. 1997. A novel cytoplasmic protein that interacts with the Ah receptor, contains tetratricopeptide repeat motifs, and augments the transcriptional response to 2,3,7,8-tetrachlorodibenzo-*p*-dioxin. *J. Biol. Chem.* 272:8878–8884.

Meyer, B.K., M.G. Pray-Grant, J.P. Vanden Heuvel, and G.H. Perdew. 1998. Hepatitis B virus X-associated protein 2 is a subunit of the unliganded aryl hydrocarbon receptor core complex and exhibits transcriptional enhancer activity. *Mol. Cell. Biol.* 18:978–988.

Mori, M., and K. Terada. 1998. Mitochondrial protein import in animals. *Biochim. Biophys. Acta.* 1403:12–27.

Neupert, W. 1997. Protein import into mitochondria. *Annu. Rev. Biochem.* 66: 863–917.

Nishi, T., F. Nagashima, S. Tanase, Y. Fukumoto, T. Joh, K. Shimada, Y. Matsukado, Y. Ushio, and Y. Morino. 1989. Import and processing of precursor to mitochondrial aspartate aminotransferase. Structure-function relationships of the presequence. *J. Biol. Chem.* 264:6044–6051.

Niwa, H., K. Yamamura, and J. Miyazaki. 1991. Efficient selection for high-expression transfectants with a novel eukaryotic vector. *Gene.* 108:193–199.

Oda, T., T. Funai, and A. Ichiyama. 1990. Generation from a single gene of two mRNAs that encode the mitochondrial and peroxisomal serine:pyruvate aminotransferase of rat liver. *J. Biol. Chem.* 265:7513–7519.

Pfanner, N., and A. Geissler. 2001. Versatility of the mitochondrial protein import machinery. *Nat. Rev. Mol. Cell Biol.* 2:339–349.

Pirkl, F., E. Fischer, S. Modrow, and J. Buchner. 2001. Localization of the chaperone domain of FKBP52. *J. Biol. Chem.* 276:37034–37041.

Terada, K., and M. Mori. 2000. Human DnaJ homologs dj2 and dj3, and bag-1 are positive cochaperones of hsc70. *J. Biol. Chem.* 275:24728–24734.

Terada, K., K. Ohtsuka, N. Imamoto, Y. Yoneda, and M. Mori. 1995. Role of heat shock cognate 70 protein in import of ornithine transcarbamylase precursor into mammalian mitochondria. *Mol. Cell. Biol.* 15:3708–3713.

Terada, K., I. Ueda, K. Ohtsuka, T. Oda, A. Ichiyama, and M. Mori. 1996. The requirement of heat shock cognate 70 protein for mitochondrial import varies among precursor proteins and depends on precursor length. *Mol. Cell. Biol.* 16:6103–6109.

Tsukamoto, T., S. Hata, S. Yokota, S. Miura, Y. Fujiki, M. Hijikata, S. Miyazawa, T. Hashimoto, and T. Osumi. 1994. Characterization of the signal peptide at the amino terminus of the rat peroxisomal 3-ketoacyl-CoA thiolase precursor. *J. Biol. Chem.* 269:6001–6010.

Wright, G., K. Terada, M. Yano, I. Sergeev, and M. Mori. 2001. Oxidative stress inhibits the mitochondrial import of preproteins and leads to their degradation. *Exp. Cell Res.* 263:107–117.

Yano, M., M. Kanazawa, K. Terada, C. Namchai, M. Yamaizumi, B. Hanson, N. Hoogenraad, and M. Mori. 1997. Visualization of mitochondrial protein import in cultured mammalian cells with green fluorescent protein and effects of overexpression of the human import receptor Tom20. *J. Biol. Chem.* 272:8459–8465.

Yano, M., M. Kanazawa, K. Terada, M. Takeya, N. Hoogenraad, and M. Mori. 1998. Functional analysis of human mitochondrial receptor Tom20 for protein import into mitochondria. *J. Biol. Chem.* 273:26844–26851.

Yano, M., N. Hoogenraad, K. Terada, and M. Mori. 2000. Identification and functional analysis of human Tom22 for protein import into mitochondria. *Mol. Cell. Biol.* 20:7205–7213.

Young, J.C., W.M. Obermann, and F.U. Hartl. 1998. Specific binding of tetratricopeptide repeat proteins to the C-terminal 12-kDa domain of hsp90. *J. Biol. Chem.* 273:18007–18010.

Young, J.C., N.J. Hoogenraad, and F.U. Hartl. 2003. Molecular chaperones Hsp90 and Hsp70 deliver preproteins to the mitochondrial import receptor Tom70. *Cell.* 112:41–50.